Evidence of Arctic-wide Atmospheric Aerosols from DMSP Visible Imagery

KEITH P. SHINE[1]

Department of Geography, University of Liverpool, United Kingdom

DAVID A. ROBINSON

Lamont-Doherty Geological Observatory of Columbia University, Palisades, NY 10964

ANN HENDERSON-SELLERS

Department of Geography, University of Liverpool, United Kingdom

GEORGE KUKLA

Lamont-Doherty Geological Observatory of Columbia University, Palisades, NY 10964

25 February 1983 and 15 March 1984

ABSTRACT

Recent work has emphasized the potential importance of atmospheric aerosols in the Arctic. This paper presents results indicating the large-scale presence of arctic aerosols during late spring. Their screening effect may be sufficient to alter significantly the shortwave radiation budget. The ratios of brightness over sea and snow covered ice surfaces are shown to be considerably lower, using DMSP shortwave imagery, than those calculated for clear skies using a radiative transfer scheme. Our analysis shows that aerosols are the most likely cause of the discrepancy. With additional calibration the method offers the potential for remote sensing of the aerosol distribution and concentration over the Arctic.

1. Introduction

The presence of aerosols in the Arctic atmosphere has been known for some time. Recently, new evidence has been presented indicating large amounts of pollution derived aerosols (e.g., Rahn and McCaffrey, 1980; Rosen *et al.*, 1981; Shaw, 1982). Preliminary studies of the effect of these aerosols on the Arctic radiation budget have been presented by Shaw and Stamnes (1980) and Porch and MacCracken (1982). The effects may be substantial.

Aerosols have been shown to be present at widely separated stations along the North American coast of the Arctic Ocean (see e.g.,Barrie *et al.*, 1981) and in the Svalbard (Heintzenberg, 1982). Local pollutants have not been found to be the major source (e.g., Radke *et al.*, 1976; Bodhaine *et al.*, 1981). There have been few *in situ* measurements of the aerosols over the Arctic Ocean itself; almost invariably, measurements have been restricted to ground level concentrations and composition at coastal sites.

Shaw (1982) and Patterson *et al.* (1982) have emphasized that ground level measurements of aerosol characteristics may not give a good indication of the bulk radiative properties in the overlying atmospheric column. The bulk properties must be established if their potential for climate perturbations is to be correctly assessed. The studies of Shaw (1975, 1982) present the only direct measurements of the vertical distribution of aerosols in the Arctic known to the authors. Pepin *et al.* (1980) have used a sun photometer onboard a satellite to measure extinction coefficients in the Arctic troposphere at the time of sunset. Recently, Freund (1983) has used routine measurements of the ground level solar radiation to infer the aerosol optical thickness for stations in the Canadian Arctic, and found that the springtime values regularly exceeded 0.1. In general, the aerosol loading drops to a summer minimum (e.g., Shaw, 1982). Springtime is particularly important from the climatic viewpoint since it is the period during which the presence of both moderate amounts of solar radiation and atmospheric aerosol will combine to give maximum impact on the radiation budget.

This note presents results pointing to the large scale presence of aerosols over the Arctic Ocean during the late spring from analyses of Defense Meteorological Satellite Program (DMSP) shortwave imagery for cloudless skies. With additional *in situ*

[1] Present affiliation: Department of Atmospheric Physics, University of Oxford, Parks Road, Oxford OX1 3PU, UK.

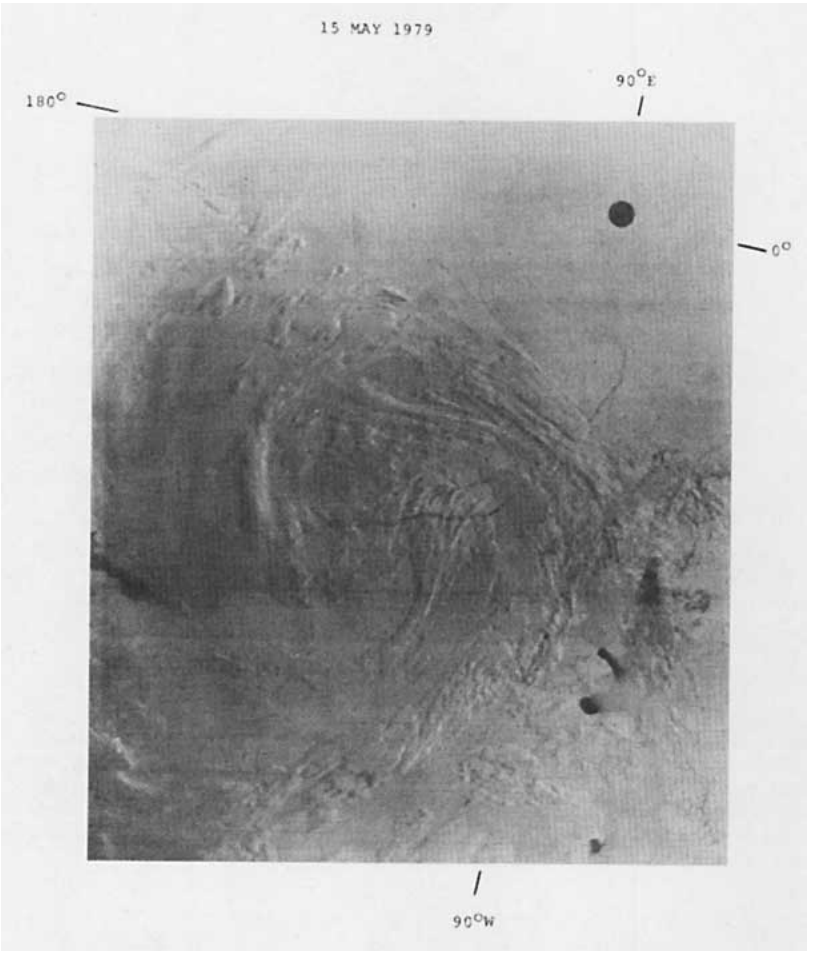

FIG. 1. DMSP image for 15 May 1979 in the region of the Canadian Arctic showing the contrast between polynyas/leads and snow covered ice/land surfaces.

atmospheric calibration, the method described here presents the potential for the quantitative analysis of Arctic aerosol loading during springtime, on a space scale hitherto impossible.

2. Analysis of DMSP imagery

The Operational Linescan System onboard DMSP satellites records solar radiation in the spectral range 0.4–1.1 μm. The use of this imagery for the detection of atmospheric aerosols has been previously shown by Fett and Isaacs (1979). The analysis presented here uses the brightness ratio between areas having distinctly different surface albedos. This method facilitates a simple extraction of data from the processed imagery. Raw radiances are not available for the DMSP sensors.

During springtime in the Arctic, the pack ice begins to break up and areas of low albedo water (as leads and polynyas) form, and contrast greatly with the surrounding snow covered ice (Fig. 1). An image processor was used to evaluate the the ratio between the brightness of the snow covered surfaces and the brightness of the polynya for a number of conditions ranging from clear to overcast skies. Snow brightness measurements were only taken over fast ice. The surface of fast ice is more homogeneous than that of pack ice because of fewer ice ridges and hummocks and subresolution fractures. The contrast between sea and snow surfaces is retained in all but thick cloud situations (Fig. 1).

Details (including position, time and solar zenith angle) of the cases studied are given in Table 1; ratios

TABLE 1. Dates, coordinates and solar zenith angles for areas at which brightness ratios were calculated.

Identification number	Date (1979)	Coordinates (deg)	Solar zenith angle (deg)
13832	15 May	74–77 N; 77–87 E	58.7
13859	17 May	75–77 N; 135–147 E	55.8
13901	20 May	76–77 N; 147–152 E	56.6
13909 (i)	20 May	70–72 N; 125–142 W	63.8
13909 (ii)	20 May	74–76 N; 80–84 W	55.6
14073	1 June	75–78 N; 80–90 E	56.4
14211	10 June	74–77 N; 120–140 E	58.7
14251	13 June	76–79 N; 108–124 E	57.1

are shown plotted against solar zenith angle in Fig. 2. All cases relate to May and early June in the region between 70 and 78°N. Only large polynyas and not leads were used in the analysis. The clear sky ratios lie in the range between 3.5 and 4.8. Since ratios in Table 1 include the highest of those analyzed, and thin cloud was found to have a large impact on the ratios, the authors are confident that the ratios were measured in a cloudless atmosphere. There are insufficient data to draw any conclusions regarding the zenith angle dependence of the brightness ratios.

3. Radiative transfer calculations

The satellite observed brightness ratios were related to calculated ratios using the 24 spectral band delta-Eddington scheme of Slingo and Schrecker (1982). The DMSP sensor response over the region 0.4–1.1 μm was incorporated from Fett (1981) and Fett and Isaacs (1979). The subarctic summer atmosphere of McClatchey *et al.* (1972) was used. When the extremes of the McClatchey tropical and subarctic winter atmospheres were used, an alteration in the calculated brightness ratio was only found in the second decimal place. Thus, the lack of knowledge of the atmospheric water vapor content presents no significant source of error.

Observations of the time of snow melt (e.g., Marshunova and Chernigovskii, 1978) show that for the time of year under consideration here, the surface of the ice is covered in snow. The calculations were performed using data from the spectral snow albedo model of Wiscombe and Warren (1980) interpolated onto the 24 spectral band grid. Two types of snow were considered: one, intended to represent clean fresh snow, has a grain radius of 100 μm; the other, aged snow, has a grain radius of 1000 μm and a soot content of 0.05 ppm. The clear sky surface albedo of the two types are 0.833 and 0.681, respectively, at a zenith angle of 66°. These two extremes bracket the actual snow surface albedos (e.g., Marshunova and Chernigovskii, 1978). Zenith angle dependence of the snow albedo was neglected; over the range of zenith angles considered, the albedo will change by less than 0.01.

Sea–surface albedos were derived using the expression given by Briegleb and Ramanathan (1982) which gives a diffuse albedo of 0.08. Over the range of zenith angles from 55.8° to 63.8°, the clear sky surface albedo ranged from 0.078 to 0.098.

The clear sky ratios between the planetary albedo over the sea and snow surfaces are shown in Fig. 2. The albedo ratios are consistently higher than those observed from the DMSP imagery. Possible reasons for this discrepancy are discussed in the next section.

4. The role of atmospheric aerosols in determining the brightness ratio

To account for the discrepancy between the observed and calculated brightness ratios, several potential explanations were assessed. By using extreme

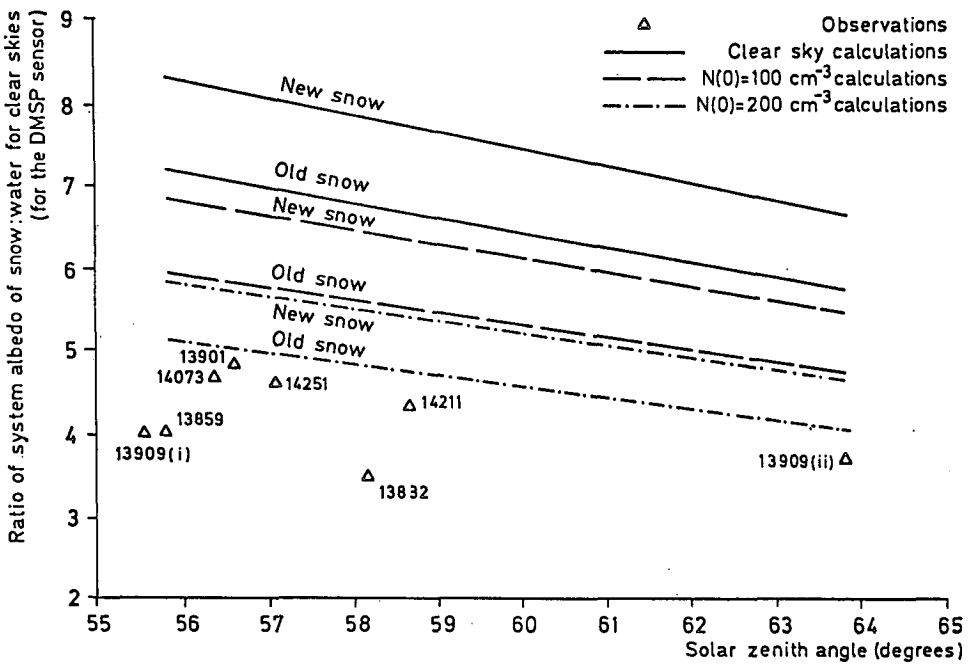

FIG. 2. Variation of ratio of the system albedo over snow to system albedo over water. Observations are marked by triangles and numbers refer to the identification number given in Table 1. Radiative transfer calculations for clear skies and two degrees of aerosol loading (see text for details) are given by the lines. Calculated values account for DMSP sensor response (Fett, 1981).

values for sea surface albedos and examining the likely error from anisotropic reflection by the earth and atmosphere, it is concluded that aerosols must be playing a major role.

a. *Surface albedos*

The range of snow albedos used in the calculations is sufficiently large to remove them as a source of the difference between observations and calculations. The data of Cogley (1979) indicate that clear sky values of sea surface albedo at these latitudes will be at most 0.1; Kondratyev (1969) also reports measurements indicating albedos of less than 0.1 for the solar zenith angles under consideration here. Any surface roughness of the water causes a further decrease in the albedo for such zenith angles. However, we do not know the percentage of subresolution floating ice in the polynyas, which would raise albedo values. For instance, if 5% of the polynya is covered with snow free ice having an albedo of 0.5, its albedo would rise to 0.12 given an open water albedo of 0.1. In order to equate our theoretically derived ratios with the observed values, it would be necessary to have a polynya surface albedo of 0.15. This would require close to 10% ice cover with the albedo of 0.65 which is not considered likely.

b. *Adjacency effects*

Close to the boundary between two surfaces with different albedos, atmospheric scatter results in radiation reflected from one surface contributing to the satellite measured radiance over the other surface. Thus, the radiance close to the ice/sea boundary will be altered such that the radiances above the snow will be decreased and those over the sea increased; this will contribute to a decrease in the brightness ratio. Kaufman and Joseph (1982) have considered this question for LANDSAT imagery. Their results show that adjacency effects are of significance only within 3–4 km of the boundary. The theoretical calculations of Mexler and Kaufman (1980) show that for a surface albedo contrast of 0.6, adjacency effects are negligible beyond 5–10 km. Our observed brightness ratios were derived from DMSP pixels well away from the ice/sea boundary (hence the choice of polynyas rather than leads). Since the DMSP resolution is about 5.6 km, problems should only be encountered for pixels immediately adjacent to the boundary and should present no significant source of error for the calculations presented here.

c. *Anisotropic reflection from the surface*

The satellite registers only a small proportion of the reflected radiation, whereas the calculations represent the radiation reflected, integrated over all angles. For surfaces which reflect radiation isotropically, this provides no problem when comparing observations and calculations. However, many natural surfaces (and in particular, water) display significant anisotropy so that a single brightness measurement may not necessarily represent the true hemispheric albedo (e.g., Taylor and Stowe, 1984).

Angular reflectance plots from the Nimbus-7 ERB experiment (Taylor and Stowe, 1984) have been used to assess the possible magnitude of any error. From the satellite viewing geometry (Fett, 1981) it can be shown that the maximum viewing zenith angle of the satellite is 61° and normally less. The angular reflectance plots of Taylor and Stowe (1984) give the bidirectional reflectance factor (BDRF) i.e., the ratio of the brightness viewed from a specific angle to the hemispheric albedo. The plots show that away from the forward scatter peak, which would show up as sunglint on the images, the BDRF varies between approximately 0.9 and 1.1 for snow surfaces at solar zenith angles of 53 and 66.4° and between 0.6 and 2.0 for sea surfaces at the same solar zenith angles. However, the azimuthal angles for which the BDRF is greater than unity over water are restricted to less than 30° either side of the forward scatter peak for a viewing zenith angle of 40°. The satellite is thus more likely to underestimate the true water albedo than the snow albedo. If the effect were to be systematic, the observed ratios would be *higher* than those calculated, not lower as was found (Fig. 2).

d. *Atmospheric aerosols*

One remaining possibility is that there are additional scattering/absorbing particles in the atmosphere that were not considered in our radiation calculations. As discussed in the Introduction, considerable quantities of aerosol have been detected in the Arctic. Qualitatively, the presence of scattering/absorbing aerosol will lower the brightness ratios. Over a dark sea surface, the additional scatterers will increase the system albedo (so that the brightness ratio will decrease even in the absence of aerosol absorption) while over a bright snow surface the additional absorbers will prevent radiation from reaching the surface to be reflected, decreasing the system albedo.

Quantitative modeling of the effect of aerosols is hampered by the paucity of data relating to the aerosols and their height distribution. In general, estimates of the aerosol scattering coefficient at different locations in the Arctic are consistent (e.g., Bodhaine *et al.*, 1981; Barrie *et al.*, 1981; Heintzenberg, 1982). A typical value for the scattering coefficient in March is 2.0×10^{-5} m^{-1}, falling an order of magnitude by June. However, measurements of aerosol absorption vary greatly. For example, Heintzenberg (1982) reports values of between 0.5 and 1.0×10^{-6} m^{-1} in March at Spitzbergen, while Rosen *et al.* (1981) and Patterson *et al.* (1982) report values

greater than 2.0×10^{-6} m^{-1} at Barrow. The discrepancy is mainly due to the different experimental techniques used to derive the absorption coefficient. Rosen *et al.* (1981) used a laser transmission method, whilst Heintzenberg (1982) used an integrating sphere photometer. Sadler *et al.* (1981) have shown that the two methods can yield absorption coefficients whereby those from the laser transmission method were some 2.5 times greater; these authors were, however, unable to say which of the two methods should be considered the most reliable. In the face of these uncertainties, quantitative modeling of the radiation field is difficult.

Nevertheless, our computations show that the aerosol loading can be of a sufficient magnitude to resolve the discrepancy between observed and calculated brightness ratios. The aerosol optical properties (single scatter albedo, extinction coefficient and asymmetry factor) were taken from Newiger and Bahnke (1981). Their aerosols with refractive indices of $M = 1.5 - 0.02$ i and $M = 1.5 - 0.003$ i were used, and the optical properties were interpolated onto the wavelength grid used in the Slingo and Schrecker (1982) radiation scheme. The more absorbing aerosol ($M = 1.5 - 0.02$ i) has an absorption coefficient that lies between the measurements of Heintzenberg (1982) and Rosen *et al.* (1981) that were previously discussed.

Late spring aerosol measurements (e.g., Barrie *et al.*, 1981; Bodhaine *et al.*, 1981; Heintzenberg, 1982) indicate that surface concentrations of aerosols between 100 cm^{-3} and 200 cm^{-3} are appropriate; this yields extinction coefficients in the range $5–10 \times 10^{-5}$ m^{-1} at 0.5 μm. The height distribution of the aerosols was taken from data given by Shaw (1975) as

$$N(z) = N(0) \exp(-z/1.35), \quad (1)$$

where z is the height (in kilometers), $N(z)$ the number concentration at height z and $N(0)$ the surface concentration of aerosols. Using $N(0) = 200$ cm^{-3}, the aerosol extinction optical depth at 0.5 μm is 0.125, which corresponds well with the observations of Shaw (1982).

The impact of aerosols on the planetary albedo over new snow and water is shown in Fig. 3, where the planetary albedo versus the cosine of the solar zenith angle for both clean and aerosol loaded skies is illustrated. The effect of a surface concentration of 200 cm^{-3} is shown. The contrast between the effect of the two aerosol types on the planetary albedo over snow emphasizes the need for accurate knowledge of the aerosol properties. The changes in planetary albedo over the different surface types are in good agreement with the results of Coakley *et al.* (1983). As discussed here, present data favor the use of the more absorbing ($M = 1.5 - 0.02$ i) aerosol.

The results shown on Fig. 3 represent planetary albedos for the entire solar spectrum. In fact, DMSP imagery enhances the brightness ratio. For example, for a cosine of the solar zenith angle of 0.3, the

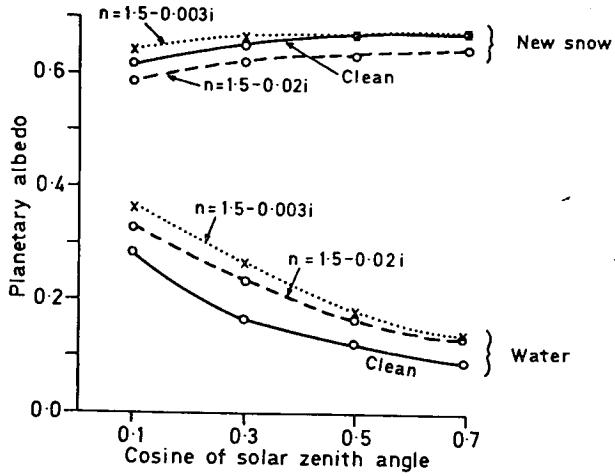

FIG. 3. Planetary albedo versus the cosine of the solar zenith angle for a cloudless subarctic summer atmosphere over water and over a new snow surface. Calculations are for a clean atmosphere and for aerosols with refractive indices of 1.5–0.003 i and 1.5–0.02 i. The surface particle concentration is 200 cm^{-3} and decreases with height as given by Eq. (1).

brightness ratio between new snow and water is 3.52 for the whole spectrum, and 4.82 for the DMSP sensor response, for clear skies. This is mainly due to the fact that the albedo of snow is highest in the region of the spectrum detected by the DMSP sensor.

The effect of the more absorbing aerosol on the snow/sea albedo ratio is shown in Fig. 2. For a ground concentration of 200 cm^{-3}, the apparent albedo, as seen by the DMSP sensor over a sea surface, would increase by 0.05 and decrease by 0.05 over snow. Comparing these results with the observations on Fig. 2, it is clear that aerosols provide an effect of sufficient magnitude to explain the difference, particularly when taking into account the uncertainties in the aerosol parameters.

Freund's (1983) estimates of aerosol optical depth in the Canadian Arctic are for a period which includes the measurements reported here, and so a limited comparison is possible. Freund used a simple radiative transfer model to estimate the surface shortwave flux, and calculated the necessary aerosol loading to account for the difference between observations and calculations. Direct comparison is not possible because Freund used a weakly absorbing aerosol (based on the measurements of Heintzenberg, 1982). Figure 3 indicates that the brightness ratio method used here will lead to larger optical thicknesses than those found by Freund. Three of the ground stations are close to points shown in Table 1. Resolute and Alert are close to ID number 13909 (ii), and Inuvik lies to the south of ID number 13909 (i). Freund gives values of the optical thickness in the range of 0.08 to 0.16 at Alert in May 1979, which agrees well with the results shown in Fig. 2. At Inuvik, however, the estimated

optical thicknesses lie between 0.03 and 0.06, somewhat lower than the value estimated here. Freund's values for Inuvik in May 1979 do seem anomalously low in comparison with his results for 1978 and 1980 and for other months in 1979.

In summary, the implication of the calculations presented here is that aerosols in the late spring appear to be an Arctic-wide phenomenon, present in sufficient quantities to alter significantly the radiation budget of the Arctic. With adequate *in situ* calibration, the method described in this paper offers the capability to expand the monitoring of the aerosol loading of the Arctic atmosphere on a scale not possible by surface measurements.

Acknowledgments. One author (KPS) was funded under NSF Subcontract ATM-80-18898 to the University of Liverpool, and two others (DR and GJK) supported by a U.S. Department of Energy Grant DE 10665. A. Slingo is thanked for making available the radiation scheme, and S. G. Warren thanked for providing unpublished snow albedo data. The helpful comments of a referee are gratefully acknowledged.

REFERENCES

Barrie, L. A., R. M. Hoff and S. M. Daggaputty, 1981: The influence of mid-latitudinal pollution sources on Haze in the Canadian Arctic. *Atmos. Environ.*, **15,** 1407–1419.

Bodhaine, B. A., M. J. Harris and G. A. Herbert, 1981: Aerosol light scattering and condensation nuclei measurements at Barrow, Alaska. *Atmos. Environ.*, **15,** 1375–1389.

Briegleb, B., and V. Ramanathan, 1982: Spectral and diurnal variations in clear sky planetary albedo. *J. Appl. Meteor.*, **21,** 1160–1171.

Coakley, J. A., R. D. Cess and F. B. Yurevich, 1983: The effect of tropospheric aerosols on the Earth's radiation budget: A parameterization for climate models. *J. Atmos. Sci.*, **40,** 116–138.

Cogley, J. G., 1979: The albedo of water as a function of latitude. *Mon. Wea. Rev.*, **107,** 775–781.

Fett, R. W., 1981: Navy Tactical Applications Guide, Volume 3. North Atlantic and Mediterranean weather analysis and forecast applications. NEPRF Tech. Report 80-07.

——, and R. G. Isaacs, 1979: Concerning causes of 'anomalous gray shades' in DMSP visible imagery. *J. Appl. Meteor.*, **18,** 1340–1351.

Freund, J., 1983: Aerosol optical depth in the Canadian Arctic. *Atmosphere: Atmos. Ocean,* **21,** 158–167.

Heintzenberg, J., 1982: Size segregated measurements of particulate elemental carbon and aerosol light absorption at remote Arctic locations. *Atmos. Environ.*, **16,** 2461–2469.

Kaufman, Y. J., and J. H. Joseph, 1982: Determination of surface albedos and aerosol extinction characteristics from satellite imagery. *J. Geophys. Res.*, **87,** 1287–1299.

Kondratyev, K. Ya., 1969: *Radiation in the atmosphere,* Academic Press, 912 pp.

Marshunova, M. S., and N. T. Chernigovskii, 1978: Radiation regime of the foreign Arctic. Office of Polar Program. NSF TT 72-51034.

McClatchey, R. A., R. W. Fenn, J. E. A. Selby, F. E. Volz and J. S. Garing, 1972: *Optical Properties of the Atmosphere (Third edition).* Air Force Cambridge Research Laboratories, Environmental Research Papers no 411, 108 pp.

Mexler, Y., and Y. J. Kaufman, 1980: The effects of the Earth's atmosphere on contrast reduction for a non-uniform surface albedo and 'two-halves' field. *J. Geophys. Res.*, **85,** 4067–4083.

Newiger, M., and K. Bahnke, 1981: Influence of cloud composition and cloud geometry on the absorption of solar radiation. *Contrib. Atmos. Phys.*, **34,** 370–382.

Patterson, E. M., B. T. Marshall and K. A. Rahn, 1982: Radiative properties of the Arctic aerosol. *Atmos. Environ.*, **16,** 2967–2977.

Pepin, T. J., R. W. Lane, F. Simon and T. A. Cerni, 1980: Remote sensing of the vertical concentration of aerosols and ozone in the Arctic atmosphere. *Proc. Int. Rad. Symp. Fort Collins, Colorado,* 35–37.

Porch, W. M., and M. C. MacCracken, 1982: Parametric study of the effects of Arctic soot on solar radiation. *Atmos. Environ.*, **16,** 1365–1371.

Radke, L. F., P. V. Hobbs and J. E. Pinnons, 1976: Observations of cloud concentration nuclei, sodium containing particles, ice nuclei and the light scattering coefficient near Barrow, Alaska. *J. Appl. Meteor.*, **15,** 982–995.

Rahn, K. A., and R. J. McCaffrey, 1980: On the origin and transport of the winter Arctic aerosol. *Ann. N.Y. Acad. Sci.*, **338,** 486–503.

Rosen, H., T. Novakov and B. A. Bodhaine, 1981: Soot in the Arctic. *Atmos. Environ.*, **15,** 1371–1374.

Sadler, M., R. J. Charlson, H. Rosen and T. Novakov, 1981: An intercomparison of the integrating plate and laser transmission methods for the determination of aerosol absorption coefficients. *Atmos. Environ.*, **15,** 1265–1268.

Shaw, G. E., 1975: The vertical distribution of tropospheric aerosols at Barrow, Alaska. *Tellus,* **27,** 39–49.

——, 1982: Atmospheric turbidity in Polar Regions. *J. Appl. Meteor.*, **21,** 1080–1088.

——, and K. Stamnes, 1980: Arctic haze: Perturbation of the polar radiation budget. *Ann. N.Y. Acad. Sci.*, **338,** 533–539.

Slingo, A., and H. M. Schrecker, 1982: On the shortwave radiative properties of stratiform water clouds. *Quart. J. Roy. Meteor. Soc.*, **108,** 407–426.

Taylor, V. R., and L. L. Stowe, 1984: Reflectance characteristics of uniform earth and cloud surfaces derived from NIMBUS-7 ERB. *J. Geophys. Res,* **39,** 4987–4996.

Wiscombe, W. J., and S. G. Warren, 1980: A model for the spectral albedo of snow. I: Pure snow. *J. Atmos. Sci.*, **37,** 2712–2733.